DispatchDate: 24.02.2022 · ProofNo: 1318, p.1

nature human behaviour

ARTICLES

https://doi.org/10.1038/s41562-022-01318-6



# Evidence integration and decision confidence are modulated by stimulus consistency

Moshe Glickman [1,2] ✉, Rani Moran [2,3,6] and Marius Usher [4,5,6] ✉

**Evidence integration is a normative algorithm for choosing between alternatives with noisy evidence. It has been successful in accounting for vast amounts of behavioural and neural data. However, this mechanism has been challenged by non-integration heuristics, and tracking decision boundaries has proven elusive. Here we first show that the decision boundary can be monitored using a model-free behavioural method termed decision classification boundary, which extracts decision boundaries by optimizing choice classification based on the accumulated evidence. Using this method, we provide direct support for evidence integration over non-integration heuristics, show that the decision boundaries collapse across time and identify an integration bias whereby incoming evidence is modulated based on its consistency with preceding information. This consistency bias, which is a form of pre-decision confirmation bias, was supported in four cross-domain experiments, showing that choice accuracy and decision confidence are modulated by stimulus consistency. Strikingly, despite its seeming sub-optimality, the consistency bias fosters performance by enhancing robustness to integration noise.**

Decisions often require the integration of multiple, potentially contradictory, pieces of evidence. Consider, for example, a judge deliberating over whether a defendant is guilty or not, or a medical doctor diagnosing a patient's disease. Extensive research has converged on the proposition that integration of evidence to a decision boundary is a normative mechanism for such evidence-based decisions. This mechanism provides the fastest mean response time (RT) for a target accuracy rate[1–4] and accounts for an impressive amount of behavioural and neural choice data (see ref. [5] for a review). For instance, integration-to-boundary models[1,6–11] provide a parsimonious account for the shape of choice–RT distributions of correct and incorrect responses as a function of stimulus difficulty, as well as for the well-known speed–accuracy trade-off[12] stating that people can improve their decision accuracy by sampling more information, and vice versa. Moreover, integration-to-boundary models are supported by the monitoring of neural activation in brain decision areas during choice tasks[13,14] (but see ref. [15]).

Despite this strong support, the evidence integration framework has been challenged by alternative non-integration mechanisms, such as heuristics based on the detection of a single high-value sample, which can account for many of these choice patterns as well[16] (see also the discussion in ref. [17]). Moreover, research within the evidence-integration framework has suggested that, in many decision environments, the reward rate is optimized when the choice threshold varies (for example, collapses) as a function of time[18,19]. Evidence for such time-varying boundaries have been found in both humans and non-human primates[20,21] (but see ref. [22]). These studies, however, have estimated the boundary whilst assuming arbitrary functional assumptions (for example, that the boundary decays according to a Weibull function). Thus, it is important to validate the integration assumption, and to monitor the decision boundary without imposing such assumptions.

A second aspect of the normative model is that the evidence (construed as the increase in the log likelihood of the two hypotheses) is integrated without biases or distortions. However, recent findings indicate a variety of biases in the sampling and weighting of evidence. Attentional biases, for example, affect the relative weighting assigned to simultaneous pieces of evidence[23–26]. Another type of decision biases are history biases, such as the confirmation bias[27–31], according to which committing to a categorical choice distorts the interpretation of subsequent information. Potential biases of this kind must be taken into account when assessing whether evidence is accumulated and when estimating decision boundaries. In turn, the decision bound can interact with the estimation of the bias itself.

Here, we addressed these issues by using a novel behavioural method that is agnostic to the (temporally) functional shape of the boundary and which we term decision classification boundary (DCB). The DCB extracts the decision boundary (at each time frame) by optimizing the classification of the agent's behaviour (that is, terminating the trial by choosing alternative A, terminating the trial by choosing alternative B or sampling more evidence), based on the evidence accumulated up to this time point. When evidence integration is perfect (that is, free of distortions and biases), the DCB recovers the decision boundary. More broadly, however, DCBs provide a novel behavioural signature—a benchmark for evaluating biases in evidence integration—and also allow us to derive a simplified behaviourally approximate bias-free model, which compensates for integration biases, via a change in the classification curve only (see Results section for further details and an example). Applying this method to data from experiments across choice domains (numerical cognition and perception), we find strong support for evidence integration over heuristic non-integration models. Furthermore, we demonstrate an important new factor modulating evidence accumulation, viz. stimulus consistency, corresponding to an increased relative weighting of pieces of evidence preceded by information supporting the same choice alternative, resulting in a type of momentary confirmation bias[28,30,31], which operates

[1]Department of Experimental Psychology, University College London, London, UK. [2]Max Planck UCL Centre for Computational Psychiatry and Ageing Research, University College London, London, UK. [3]Wellcome Centre for Human Neuroimaging, University College London, London, UK. [4]School of Psychology, University of Tel Aviv, Tel Aviv, Israel. [5]Sagol School of Neuroscience, University of Tel Aviv, Tel Aviv, Israel. [6]These authors jointly supervised this work: Rani Moran, Marius Usher. ✉e-mail: mosheglickman345@gmail.com; marius@tauex.tau.ac.il

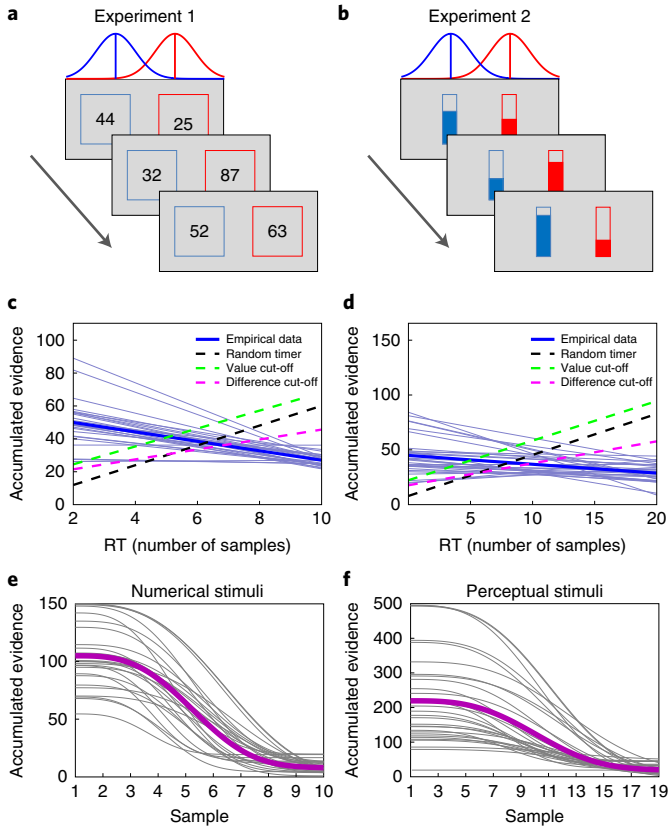


**Fig. 1 | Experimental paradigms and behavioural signature of integration to boundary. a**,**b**, Experimental paradigms. Participants are presented with pairs of numerical values (**a**, experiment 1) or bars (**b**, experiment 2) sampled from two overlapping Normal distributions and are asked to choose which sequence was drawn from a distribution with a higher mean value (experiment 1) or greater mean length (experiment 2). The presentation is terminated by the decision of the participant (that is, a free response protocol). **c**, The accumulated evidence of all participants (thick blue line) as a function of decision time. Thin blue lines correspond to accumulated evidence of individual participants. Dashed black, green and magenta lines correspond to the random time model, and to the value and difference heuristics, respectively. **d**, As in **c** but for experiment 2. **e**,**f**, The collapsing boundaries obtained in experiment 1 (**e**) and 2 (**f**). Thick purple lines correspond to the boundaries generated using the group mean parameters. Grey lines correspond to the boundaries of individual participants.

during (rather than after) a decision. Importantly, this mechanism contributes to decision quality, by increasing the robustness to late (non-encoding) noise[32,33].

We start with a description of our experimental design (showing it is possible to extract behavioural signatures of integration to boundary), followed by a computational section that presents the DCB method. We then apply this method to the data from two cross-domain experiments, focusing on the dependence of the DCB on stimulus consistency, and resort to computational modelling to specify the stimulus-consistency mechanism. We then present the results of two additional experiments designed to validate the predictions of this mechanism. Finally, we examine whether and under which conditions the stimulus-consistency mechanism can foster performance.

## Results

**Experimental design and signature of integration to boundary.** In two experiments (experiment 1, reported in ref. [34], and experiment 2, novel data), participants were presented with sequences of pairs of stimuli (two-digit numbers or bars, respectively; Fig. 1a,b) sampled from two overlapping Normal distributions (Experimental methods). The sequences were presented at a rate of 2 pairs per second (numbers) and 5 pairs per second (bars), and were terminated by the participant's response. The task was to select the sequence that corresponded to the distribution generating the higher mean (red Gaussian in Fig. 1a,b). In experiment 2, participants were also asked to reported their degree of confidence for each choice. Between trials, we manipulated stimulus difficulty by varying the separation between the Normal distributions (see Experimental methods section for further details). In total, 27 participants performed 500 trials in experiment 1 and 30 participants performed 480 trials in experiment 2.

In previous work, we showed that the choices in experiment 1 (numerical evidence) support integration of evidence to a collapsing boundary and excluded a set of non-integration models[34]. Here, we extend this analysis to the data in the perceptual domain (experiment 2). The thick blue lines (group data) and thin grey lines (individual subjects) in Fig. 1c,d are obtained by integrating the trial-by-trial stimulus evidence (that is, computing the cumulative sum of differences between the sequence pairs of samples) until the decision moment, and averaging across trials for each RT. These lines show a mildly decreasing pattern (Fig. 1c: $b=-2.86$, $t_{\text{against }0}=-7.08$, $P<0.001$, 95% CI −3.65 to −2.07; Fig. 1d: $b=-0.86$, $t_{\text{against }0}=-3.18$, $P=0.001$, 95% CI −1.40 to −0.33), which is the behavioural signature of integration to a collapsing boundary (for further details, see ref. [34] and Supplementary Fig. 1). These results are consistent with previous findings that accumulated evidence decreases with RT[35–37], as well as with model fitting results using a Weibull parametrization of the boundary[38], which also indicates a collapsing boundary (Fig. 1e,f). Critically, the descending slopes of integrated evidence rule out non-integration strategies such as (1) random timer, in which the RT is determined by a process that is exogenous to the integration of evidence (dashed black line), (2) value cut-off, in which observers choose the sequence in which a number exceeding some predetermined threshold first appears (dashed green line) and (3) difference cut-off, in which observers choose based on the first frame in which the difference between the numbers exceeds a predetermined threshold (dashed magenta line). All of these non-integration models predict that the integrated evidence increases (rather than decreases) with the number of samples (see Computational methods section for further details about these strategies). This is because, if the stopping rule is independent of the integrated evidence, longer decision trials necessarily accumulate more evidence. Whilst these results provide support for integration to boundary, the actual shape of the boundary trajectory (Fig. 1e,f) is only extracted via model fitting (note that the actual boundary is not linearly decreasing with time), as the evidence-integration lines (Fig. 1c,d, blue and thin grey lines) are systematically biased by the accumulation of noise during the trial[34]. In the following, we present a model-free method to estimate the decision boundary via a classification boundary curve. It is more robust to accumulation noise and reconstructs the actual shape of the decision boundary.

**Model-free extraction of decision boundaries.** We simulated synthetic data based on the experimental task we used in our experiments (Fig. 1a,b and Computational methods), in which sequences of values are sampled from two overlapping Normal distributions. It is assumed that the subjects integrate a noisy version of the evidence at each frame, according to the following difference equation:

$$X(t) = X(t-1) + \mu(t) + \varepsilon(t), \varepsilon \sim N\left(0, \sigma^2\right), \quad (1)$$

where $X(t)$ is the accumulated differences between the sequences at time $t$, $\mu(t)$ is the difference between the samples at time $t$ and $\varepsilon(t)$ is a temporally independent random internal Gaussian noise

generated, which is independent from the evidence-sampling noise (Fig. 1a,b). Note that, unlike $\epsilon(t)$, $\mu(t)$ is directly available to the experimenter. We also assumed that a response is triggered when the integrated noisy evidence reaches one of two symmetric decision boundaries. Two types of boundaries were used in these simulations: fixed and collapsing[38]. For the collapsing boundary, we follow ref. [38] and parametrize the boundary using Weibull functions (Computational methods). In each simulation, we ran 10,000 trials in which values sampled from the two distributions were integrated with additional internal noise. For each trial, we recorded the choice, as well as the input sequences (without the internal noise) sampled until a decision was made.

Based on these data, we reconstruct the boundary at each time frame using a method based on linear discriminant analysis[39,40] (LDA), which generates boundary classification curves. These curves are obtained by applying LDA to the integrated evidence excluding the random internal noise, defined as

$$Y(t) = Y(t-1) + \mu(t). \quad (2)$$

The LDA was applied to the integrated evidence ($Y(t)$) of the observer at each time frame, so as to classify the action at each time frame to one of three categories: choose alternative A (Fig. 2a,b, blue distributions), choose alternative B (Fig. 2a,b, green distributions) or continue sampling (Fig. 2a,b, pink distributions). The classification boundary curve (Fig. 2a,b, red line) best separates the different classes (Computational methods section and Table 1). Note that, for each time frame ($t$), the LDA was applied to all trials in the experiment that were not terminated before the $t$-th frame. In addition, note that in the absence of internal noise, the true decision boundary would separate these categories perfectly. However, in the presence of internal noise, which may increase the values of integrated evidence that lie below the boundary (blue areas), or vice versa (pink areas above the boundary), there is some unavoidable overlap.

The results are illustrated in Fig. 2a,b, which shows that the DCBs (solid red lines) recover quite accurately the generating boundaries (dashed black lines). In particular, the extracted boundary is temporally constant or decreases as a function of time, when the generating boundary is flat or collapsing, respectively. Notably, the quantitative agreement between the generating and recovered boundaries is high. Note that the model-free boundary extraction method makes no a priori parametric assumptions about the shape of the model boundary. As shown in Fig. 2c,d, for synthetic data generated using the non-integration-to-boundary, that is, value (or difference) cut/off heuristics, the three distributions of evidence (trials in which the model continues sampling (pink) and trials in which response has been made (blue and green)) show substantial overlap. Consequently, the decision classification curve algorithm fails to correctly classify the three classes of trials based on the integrated evidence. Thus, the presence of an accurate boundary classification curves (Fig. 2a,b) provides strong support against (non-integration) cut-off models.

In both our datasets, we find stable classification curves (see Fig. 2e,f, red lines, for representative example subjects) that imply a collapsing boundary, which are consistent with model fitting (Fig. 2e,f, dotted black line), but make no parametric assumption on the form of this boundary (see Supplementary Figs. 2 and 3 for the DCB of all participants). Finally, we linked the DCB to the basic behavioural measures of RT and accuracy. We found a high correlation between the area under the DCB and mean RT across participants, in both experiment 1 ($r=0.96$, $P<.001$; Fig. 2g) and experiment 2 ($r=0.8$, $P<0.001$; Fig. 2h). Correlations between the area under the DCB and accuracy were also found. However, they were weaker and less consistent (experiment 1: $r=0.41$, $P=0.03$; experiment 2: $r=0.29$, $P=0.1$) (Supplementary Fig. 4). Note that, although the correlation between RT and DCB is high, they are not interchangeable. An increased RT could also be caused by a reduction of the drift rate or by an increase in boundary without a time-collapsing shape.

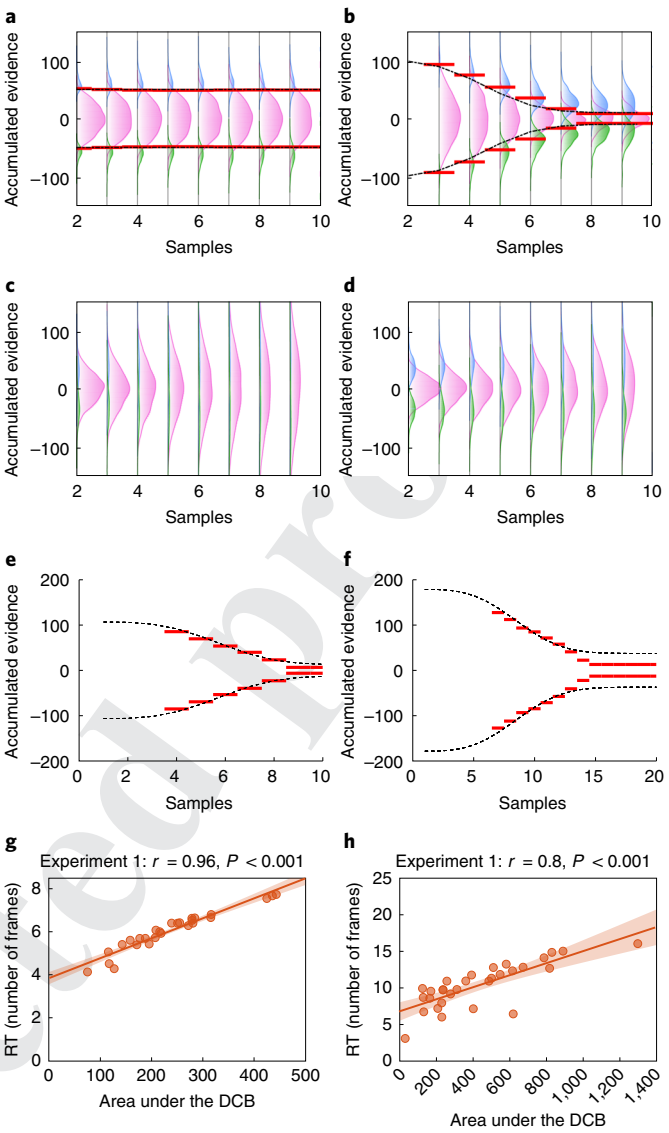


**Fig. 2 | Model-free extraction of the decision boundaries. a**,**b**, Illustration of the boundary extraction for a decision simulated using a diffusion model with fixed (**a**) or collapsing boundary (**b**). The dashed black line corresponds to the original boundary with which the model was simulated, and the red lines correspond to the model-free best-fitted DCB. The pink distributions correspond to data points within each trial in which the simulated participant continued sampling, whilst the blue and green distributions correspond to frames in which trials were terminated. The total area under the pink, blue and green distribution was normalized for each frame. **c**,**d**, Same as **a** and **b**, only for data that were simulated using the value cut-off (**c**) and difference cut-off heuristics (**d**). **e**,**f**, Experimental data of a representative subject who participated in the numerical (**e**) and perceptual experiments (**f**). Dashed black line corresponds to the model-based best-fitted boundaries, and the red lines correspond to the model-free best-fitted boundaries of the experiments. **g**,**h**, Correlations between the area under the DCB and the mean RTs across participants in experiment 1 (**g**, $r=0.96$, $P<0.001$) and experiment 2 (h, $r=0.8$, $P<0.001$).

**Table 1 | Illustration of the data used by the LDA algorithm**

| $Y(t)$ | $t$ | Response classification |
|---|---|---|
| $Y_{\text{trial }1}(t=n)$ | $n$ | Choose B |
| $Y_{\text{trial }3}(t=n)$ | $n$ | Continue sampling |
| … | … | … |
| $Y_{\text{trial }1}(t=n-1)$ | $n-1$ | Continue sampling |
| $Y_{\text{trial }2}(t=n-1)$ | $n-1$ | Choose A |
| $Y_{\text{trial }3}(t=n-1)$ | $n-1$ | Continue sampling |
| … | … | … |
| $Y_{\text{trial }1}(t=1)$ | 1 | Continue sampling |
| $Y_{\text{trial }2}(t=1)$ | 1 | Continue sampling |
| $Y_{\text{trial }3}(t=1)$ | 1 | Continue sampling |
| … | … | … |

The LDA classifies each frame to one of three classes: terminating the trial by choosing alternative A, terminating the trial by choosing alternative B or continue sampling more evidence, based on the time point ($t$) and the evidence accumulated up to this time point ($Y(t)$).

So far, we have illustrated that the DCB can accurately reconstruct the decision boundary in the case of perfect evidence integration. In the next section, we extend these results to the case in which the integration process is biased. We will show that, even then, the DCB can achieve three targets: (1) to indicate the presence of a bias, (2) to determine the simplest bias-free behaviourally equivalent model (see Supplementary Fig. 5 for an illustration for the case of leaky integration, in which the DCB compensates for the evidence loss by a change only in the decision classification line) and (3) to obtain the actual boundary in the case of a biased integration process, by selecting between a family of DCBs based on maximizing their classification performance metrics (see Supplementary Fig. 6 for further details).

**Evidence integration is modulated by stimulus consistency.** A more detailed examination of the choice data in both experiments shows that stimulus consistency, operationalized as the absolute value of the difference between the number of frames with evidence favouring each alternative divided by the total number of frames in the trial (denoted as the difference in evidence directions (DED)), has a critical impact on choices and RT, above and beyond the effect of total evidence. To illustrate this, consider two trials with the same total evidence: trial 1 (2, 3, 1, 4, total evidence 10) and trial 2 (6, −1, 8, −3, total evidence 10). Whilst both trials have a total evidence of 10 in favour of one of the alternatives, the evidence stream is more consistent in trial 1 (with a consistency measure of $\frac{4-0}{4}=1$) compared with trial 2, where half of the evidence favours one alternative whereas the other half favours the other (with a consistency measure of $\frac{2-2}{4}=0$). Previous research has shown that stimulus consistency modulates decision confidence[41]. Here, we examine its impact also on accuracy and RT. To this end, we conducted several mixed-model regression analyses (logistic for accuracy and linear for RT and confidence), in which we predicted trial-by-trial choice accuracy, RT and confidence, using accumulated evidence and stimulus consistency (defined based on the evidence stream up to subject-initiated trial completion) as fixed factors and participants as random intercepts. The results (Table 2) indicate that stimulus consistency improves accuracy and confidence and reduces RT, independent of the accumulated evidence.

Note that the DED is only one measure of stimulus consistency. More complex forms that include temporal factors can also be constructed. For example, the consistency bias may correspond to the size of the larger temporal cluster (LTC) with evidence in the same direction (that is, the largest cluster of evidence; see Supplementary Table 1 for analysis showing that such an LTC measure also predicts differences in accuracy, RT and confidence, independent from total evidence).

**DCB modulation by stimulus consistency and model comparison.** Motivated by the results above, we examined whether stimulus consistency (DED) modulates the DCB. To this end, we extracted the DCB of each frame whilst including the consistency measure (DED) as a predictor in the LDA model. Additionally, similar to the regression models above, we also included the mean evidence as a predictor in the model. We predicted that, if participants overweight consistent pieces of evidence, then less evidence will be required to reach a decision as consistency increases. Figure 3a,b shows that this was indeed the case in experiments 1 and 2: as the consistency of the evidence increased, the DCB decreased (blue line), compensating for the bias in the evidence-integration process by setting a classification curve which is lower than the original boundary (orange line).

Note that this analysis does not provide a causal explanation for how consistency affects the evidence-integration process, but rather shows that it was biased by stimulus consistency (see Discussion for details). This is because the DCB, as we showed so far, provides us with a behaviourally approximate (simpler, that is, without bias) model (Supplementary Fig. 5). To provide a more mechanistic account, we will use two complementary methods and show that they converge to the same result. We will first rely on conventional model comparisons techniques to select a model that provides the best fit for the data. Second, we will use a method developed to extract the decision boundary using the DCB in case of biased integration process (Supplementary Fig. 6). Using this method, we compare between a model assuming consistency bias and a model which does not.

First, to specify the evidence-integration mechanism, we carried out a quantitative model comparison for each participant, using AIC as a measure of fit to include a model-complexity cost. Q8 We started with the perfect integration model (which assumes no systematic distortion of the evidence a subject integrates in each frame, that is, integration is only corrupted by additive noise). Next, we examined a selective-integration (SI) mechanism that amplifies or diminishes, respectively, the stronger or weaker evidence within each frame across the two evidence streams[33,42] (Computational methods). Critically, we also examined several variants of a stimulus-consistency model. In the simplest variant, the evidence is modulated solely based on whether evidence from the preceding frame is consistent (that is, it points in the same direction) with the current frame. In a slightly more complex variant, the modulation magnitude increases linearly with the number of consistent frames and resets to baseline (no modulation) with every swap (here, we report only the results of the more complex version, which provided a better fit for the data). Finally, we also examined a preference-consistency model wherein incoming evidence is modulated based on consistency with the total integrated evidence (thus reflecting momentary preference) up to that time point (see Computational methods section for details).

In each model, we allowed for collapsing boundaries, which as illustrated in Fig. 2c,d, capture well the shape of the decision boundary (and provide much better fits to the data compared with fixed boundaries[34]). Figure 3c,d shows the group and individual participant fit measures for four models: full integration, SI, preference consistency and stimulus consistency in experiments 1 and 2. As illustrated, the most successful of the models was the stimulus-consistency version in which evidence increased at each consecutive frame in the same direction, followed by the SI model.

Finally, we developed a method to extracted the boundary using the DCB in the case of a biased integration process

**Table 2 | Beta coefficients for predicting accuracy, RT and confidence in experiments 1 and 2**

| | *β* (s.e.) | *t* | *P* | 95% CI |
|---|---|---|---|---|
| Experiment 1 | | | | |
| Accuracy | | | | |
| Evidence | 1.72 (0.06) | 28.03 | <0.001 | 1.60 to 1.84 |
| Stimulus consistency | 0.26 (0.05) | 5.69 | <0.001 | 0.17 to 0.35 |
| RT | | | | |
| Evidence | −0.26 (0.01) | −28.23 | <0.001 | −0.28 to −0.24 |
| Stimulus consistency | −0.14 (0.01) | −14.90 | <0.001 | −0.16 to −0.12 |
| Experiment 2 | | | | |
| Accuracy | | | | |
| Evidence | 0.56 (0.03) | 16.91 | <0.001 | 0.49 to 0.62 |
| Stimulus consistency | 0.27 (0.03) | 9.40 | <0.001 | 0.21 to 0.33 |
| RT | | | | |
| Evidence | −0.16 (0.008) | −20.42 | <0.001 | −0.18 to −0.15 |
| Stimulus consistency | −0.14 (0.008) | −16.78 | <0.001 | −0.15 to −0.12 |
| Confidence | | | | |
| Evidence | 0.13 (0.01) | 12.14 | <0.001 | 0.11 to 0.15 |
| Stimulus consistency | 0.15 (0.01) | 13.96 | <0.001 | 0.12 to 0.17 |

Results of mixed-model logistic regression for predicting accuracy (experiments 1 and 2) and mixed-model linear regressions for predicting RT (experiments 1 and 2) and confidence (experiment 2) using accumulated evidence and stimulus consistency as fixed factors and participants as random intercepts.

(Supplementary Fig. 6). This method uses a mixture of parametric and non-parametric methods. The former is used to characterize the biased integration process (but not the decision boundary), whilst the latter is used to extract the boundary using the DCB. To apply this method, a candidate biased integration model (for example, stimulus-consistency bias) is first selected. Then, instead of using the actual (unbiased) evidence to estimate the DCB, it is extracted based on the biased evidence (generated by simulating the biased integration model with different values of the bias parameter). For each level of the bias parameter, the DCB as well as a classification performance metric (for example, the F1 score) are computed. This results in a family of DCB curves, one for each value of the bias parameter. The bias parameter and corresponding DCB which maximizes accuracy (or any other performance metrics) comprise the estimate (see Supplementary Fig. 6 for further details and simulations). A bias parameter that equals 0 indicates that there was no bias in the evidence integration process (that is, full integration model), whereas a parameter higher than 0 indicates that the integration process was biased. Using this method, we found that the bias parameter was higher than 0 for 81% of the participants in experiment 1 (mean bias parameter 2.26, 95% CI 1.70–2.86) and for 90% of the participants in experiment 2 (mean bias parameter 4.23, 95% CI 2.76–5.90), suggesting that, in both experiment 1 and 2, the integration process was biased by the consistency of the evidence.

**Experiments 3 and 4: testing the stimulus-consistency effects.** Because in our first two experiments participants' choices terminated the information stream, trial consistency depended, at least partially, on participants' responses and was not completely orthogonal to the integrated evidence. To address this limitation, and to directly test the impact of stimulus consistency on evidence-based choice and on decision confidence, two additional experiments were designed. In both, the number of samples was fixed and the stimulus consistency was manipulated completely independently from the total evidence. In experiment 3, sequences of eight number pairs were presented at a rate of 2 Hz (as in experiment 1) and participants were instructed to choose at the end of the presentation the sequence with higher average (Fig. 4a). For each set of samples, we generated two paired trials, which consisted of the very same evidence content (across the eight time frames) for each sequence and differed only in the temporal order of the values (that is, the paired trials varied in how the values on each side were shuffled). In the consistent trial condition (Fig. 4c, bottom panel), one evidence stream provided stronger evidence in seven out of the eight frames, whereas in the inconsistent trial condition (Fig. 4c, upper panel), each stream provided stronger evidence in four frames. In addition to consistency, the difficulty of the trials was also manipulated by sampling values from $X \sim N(52, 10^2)$ and $Y \sim N(48, 10^2)$ for the difficult condition and from $X \sim N(52, 10^2)$ and $Y \sim N(44, 10^2)$ for the easy condition. In experiment 4, the stimulus-consistency effect was generalized to a much faster presentation rate of 12.5 Hz and to a single stream of evidence. Participants were presented with a sequence of eight arrays of red and blue dots (Fig. 4b) and were instructed to determine whether more of the blue or the red dots were presented in total (see ref. [43] for a similar paradigm). The number of dots presented in each frame was sampled from a Normal distribution (corresponding to the differences between the left and right distributions in experiment 3): $X \sim N(2, 20^2)$ for the difficult trials and $X \sim N(5, 20^2)$ for the easy trials. As in experiment 3, in the consistent condition, seven out of the eight frames provided support for one of the alternatives and in the inconsistent condition each alternative was supported by four of the frames. Critically, consistency and difficulty were manipulated completely orthogonally.

As shown in Fig. 5a,d, the participants were both more accurate and more confident in consistent trials than in inconsistent trials, for both the easy and the difficult conditions, in experiment 3 (accuracy/easy: permutation test $P<0.001$, Cohen's $d=1.26$, 95% CI 0.06–0.13; accuracy/difficult, permutation test $P<0.001$, Cohen's $d=1.40$, 95% CI 0.11–0.20; confidence/easy: permutation test $P<0.001$, Cohen's $d=1.11$, 95% CI 0.07–0.14; confidence/difficult: permutation test $P<0.001$, Cohen's $d=0.94$, 95% CI 0.04–0.10) and experiment 4 (accuracy/easy: permutation test $P<0.001$, Cohen's $d=1.69$, 95% CI 0.12–0.18; accuracy/difficult: permutation test $P<0.001$, Cohen's $d=2.19$, 95% CI 0.22–0.31; confidence/easy: permutation test $P<0.001$, Cohen's $d=1.56$, 95% CI 0.11–0.19; confidence/difficult: permutation test $P<0.001$, Cohen's $d=1.49$, 95% CI 0.11–0.19). Interestingly, in both experiments, the modulation of the confidence responses was different for correct and incorrect responses. Whereas for correct responses, confidence increases with stimulus consistency in experiment 3 (correct/easy: permutation test $P<0.001$, Cohen's $d=0.94$, 95% CI 0.05–0.13; correct/difficult: permutation test $P<0.001$, Cohen's $d=0.80$, 95% CI 0.03–0.10) and experiment 4 (correct/easy: permutation test $P<0.001$, Cohen's $d=1.58$, 95% CI 0.11–0.18; correct/difficult: permutation test $P<0.001$, Cohen's $d=1.41$, 95% CI 0.11–0. 18), this pattern was not obtained for incorrect trials in experiment 3 (incorrect/easy: permutation test $P=0.53$, Cohen's $d=-0.14$, 95% CI −0.05 to 0.02; incorrect/difficult: permutation test $P=0.96$, Cohen's $d=0.01$, 95% CI −0.03 to 0.03) or experiment 4 (incorrect/easy: permutation test $P=0.19$, Cohen's $d=-0.29$, 95% CI −0.14 to 0.01; incorrect/difficult: permutation test $P=0.37$, Cohen's $d=-0.20$, 95% CI −0.11 to 0.03). These findings indicate that meta-cognitive accuracy (confidence resolution = $\text{confidence}_{\text{corrects}} - \text{confidence}_{\text{errors}}$) increases with stimulus consistency in experiment 3 (resolution/easy: permutation

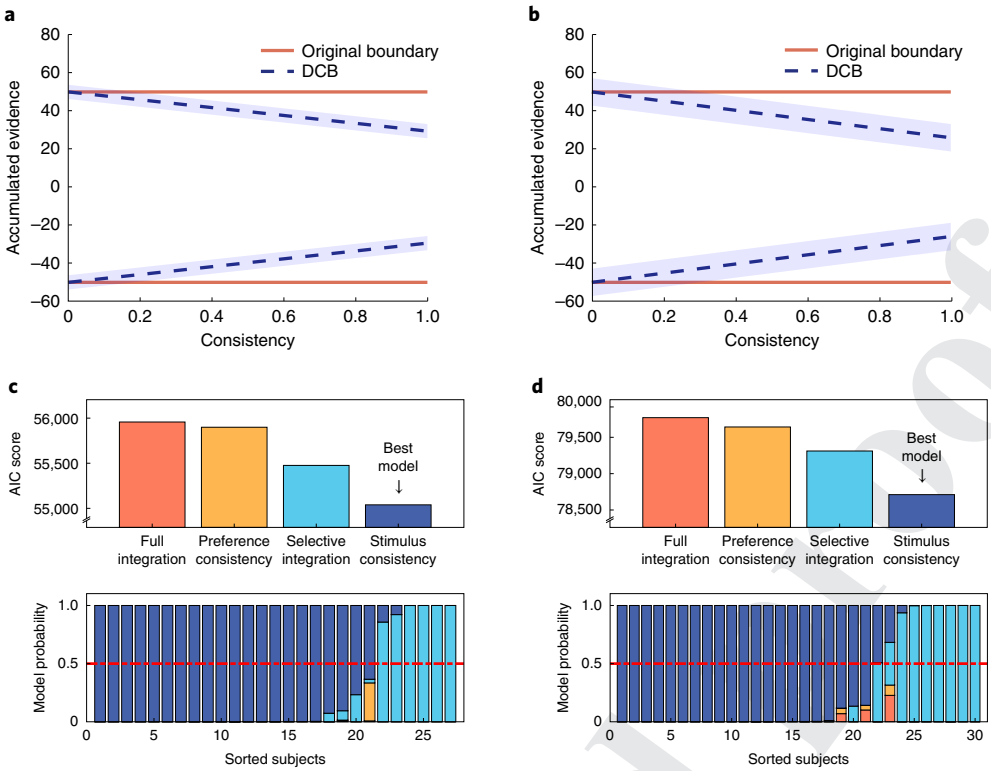


**Fig. 3 | Results of experiments 1 and 2. a**,**b**, Modulation of the DCB as a function of consistency in experiment 1 with numerical stimuli (**a**) and experiment 2 with perceptual stimuli (**b**). In the case of a stimulus-consistency bias, the weight of consistent evidence is increased, thus less evidence is required to reach a decision. The DCB (dashed blue line) compensates for that by decreasing the classification curve with consistency, and having lower values compared with the original boundary (in orange). Note that, here, we used an arbitrary boundary value for illustration purposes and that the modulation of the DCB is averaged across participants. **c**, Upper panel: the AIC group scores of the full-integration (orange), preference-consistency (yellow), SI (light blue) and stimulus-consistency (dark blue) models in experiment 1 with numerical stimuli. Lower panel: model probabilities for the individual participants. Colour coding is the same as in the upper panel. **d**, As in **c**, only for experiment 2 with perceptual stimuli.

test $P<0.001$, Cohen's $d=0.82$, 95% CI 0.05–0.16; resolution/difficult: permutation test $P=0.01$, Cohen's $d=0.59$, 95% CI = 0.02–0.11) and experiment 4 (resolution/easy: permutation test $P<0.001$, Cohen's $d=0.82$, 95% CI 0.10–0.29; resolution /difficult: permutation test $P=0.001$, Cohen's $d=0.73$, 95% CI 0.09–0.27). As shown in Fig. 5c,d (see also Supplementary Fig. 11), this effect can also be accounted for by the stimulus-consistency model by applying a signal-detection confidence approach.

We conducted quantitative model comparison for the several types of integration models using the data from experiments 3 and 4. Since the data of experiment 3 showed a recency pattern, we used leaky[10,44,45] instead of full integration as our default model for that experiment (Computational methods). Overall, we compared the following models: (1) leaky/full-integration models, in which there is no distortion of the integrated evidence other than the decaying temporal weights, (2) SI model, which, additional to integration leak, gives higher weight to high values compared with low values, within each frame (note that, as only one stream of evidence was presented in experiment 4, the SI model (which assumes weighting based on the comparison between pairs of samples) was excluded from the model comparison of that experiment) and (3) stimulus-consistency model (from experiments 1 and 2; Fig. 3c,d). The results show that the stimulus-consistency model outperformed the other models, in both experiment 3 and 4, and provides the best account for the data at group levels as well as for the majority of participants (Fig. 5e,f).

Interestingly, whereas both of the bias models are able to account for the modulation of accuracy by stimulus consistency in experiment 3 (Fig. 4c), the stimulus-consistency model accounts for subtler temporal clustering effects in the data. For example, unlike the SI model, the stimulus-consistency model predicts that accuracy is modulated by the size of the largest cluster of evidence consistent with the correct choice (LTC; see Supplementary Table 1 for the impact of this measure in experiments 1 and 2 and Supplementary Fig. 10 for data showing an association between the LTC enhancement and the advantage of stimulus consistency over the SI model in experiment 3).

**Stimulus consistency and normativity.** Why do participants increase the relative weighting of pieces of evidence that are consistent with previous ones? At face value, this distortion introduces a gap between the accumulated and 'real' evidence and should reduce task performance. Indeed, this is the case in the absence of (or for low) integration noise. As illustrated in Fig. 6a,b, however, in the presence of high integration noise, the consistency modulation makes the mechanism more robust to the corrupting impact of this noise (see the cross-over between the red and light blue lines in Fig. 6a, so that, for each level of noise, there is a consistency modulation that optimizes performance; Fig. 6B, black dots; Fig. 6A, dark-blue line). A similar robustness effect due to SI was reported for the SI model[33,42] (see also ref. [42]). In both cases, the integration mechanism distorts the actual evidence by shifting the distribution of accumulated evidence towards the correct side (see the centre of the blue/red Gaussians in Fig. 6c,d, whilst also making this distribution broader). Whilst for low noise this is detrimental to performance, for high noise it is beneficial, as the shift helps to

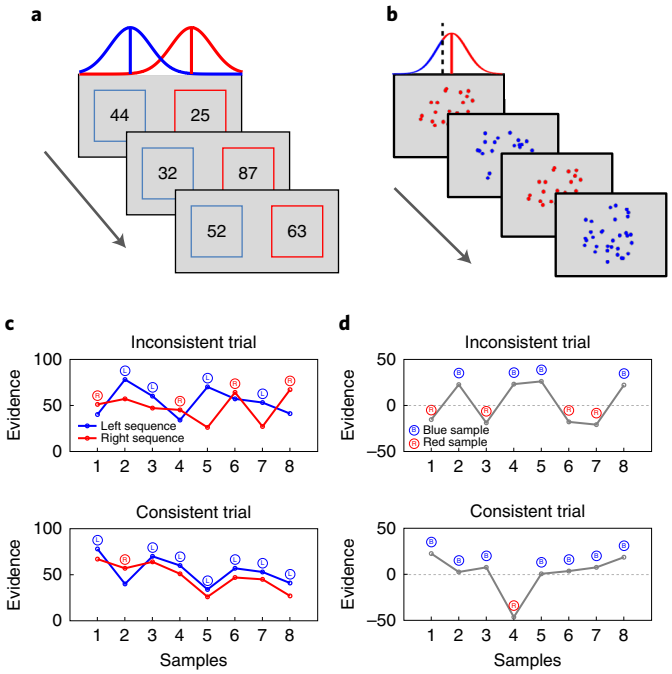


**Fig. 4 | Experimental paradigms in experiments 3 and 4. a**, Participants in experiment 3 were presented with pairs of numerical values sampled from two overlapping Normal distributions (as in experiment 1) and were asked to choose which sequence was drawn from a distribution with a higher mean. The presentation was terminated after eight pair values (that is, an interrogation protocol). **b**, Participants in experiment 4 were presented with a single stream of eight arrays of blue and red dots and were asked to indicate whether more blue or red dots were presented in total. The dashed black line indicates a value of 0. **c**, Illustration of consistent and inconsistent trials in experiment 3. Note that both trials have exactly the same amount of evidence. 'L' and 'R' symbols correspond to momentary advantages of the left or right sequences, respectively. **d**, Illustration of consistent and inconsistent trials in experiment 4. 'R' and 'B' symbols correspond to red and blue samples, respectively. As in experiment 3, both trials have exactly the same amount of evidence.

make the effect of additional noise less pronounced. Note that, since we are looking at normative considerations, the current simulations exclude integration leak. Adding it to all models does not change any of the results.

## Discussion

In the present study, we examined the mechanism that human observers deploy when making decisions on rapid streams of (perceptual and numerical) stochastic evidence. Using a behavioural model-agnostic method (the DCB curve), we showed that decision-making is well characterized by integration to boundary rather than by non-integration heuristics, and that the boundary collapses with the passage of time (Fig. 2e,f; see also ref. [46]). Furthermore, we found that DCB curves constitute an informative behavioural benchmark for evaluating biases in evidence integration. In particular, they provide a simplest bias-free evidence integration model that approximates a biased integration model (Supplementary Fig. 5). The covariation of the DCB with stimulus consistency (Fig. 3a,b) indicates a consistency bias in the evidence integration.

The DCB receives as input the integrated evidence excluding internal noise (equation (2)). As a result, its success in recovering the decision boundary is limited to experimental designs in which stimulus variability is high enough compared with internal noise. Consequently, the DCB method becomes less reliable when the presentation rate becomes closer to the integration time constant (which we assume to correspond to about 30 ms (refs. [47,48])). Supplementary Fig. 7 shows the results of a simulation examining the accuracy of the DCB method as a function of presentation time. As shown, the boundary reconstruction error increases as the presentation time decreases. This occurs because, when the evidence samples are presented close to the visual integration time scale, the neural responses to the consequent sample become fused and therefore the stimulus variability is decreased. Whilst this could make the method difficult to apply to some prominent tasks such as randomly moving dots[49,50], we believe that a rate of 5–12.5 Hz (as used here) is reasonable for most ecological tasks in which subjects make decisions based on stochastic sequences of evidence[43,51] and which sets the evidence integration at the cognitive rather than the perceptual level.

Motivated by previous studies, we examined here two types of evidence-integration biases. The first is an attention bias, which affects the relative weight of evidence given to temporally simultaneous sources of evidence[26]. In the SI model, for example, the higher of the two values presented on each frame receives a higher weight than the lower one[23,52,53]. The second bias involves the sequential impact of a frame on subsequent frames, whereby evidence that is consistent with previous frames receives higher weight than inconsistent evidence. Model comparisons supported the consistency bias in accounting for our data. Notably, consistency affected not only decision accuracy but also decision confidence[41], such that consistent evidence facilitated high decision confidence even after controlling for the total amount of evidence. Critically, consistency did not merely exert a biasing influence on confidence but also improved participant's meta-cognitive performance as measured by the resolution of confidence (that is, the correlation between confidence and choice correctness). Indeed, confidence as a function of consistency increased for correct choices but remained constant for incorrect choices. An open question for future studies is whether the effects that consistency exerts on choice accuracy and meta-cognition are dissociable.

Previous research has reported sequential effects operating at the trial level. For example, a choice biases the interpretation of evidence in subsequent trials[54–56]. Similarly, a preliminary decision biases processing of additional post-choice evidence towards confirming the initial decision[28,31,57], and decisions bias the strength evaluation of pro-choice evidence that led to it[58–60]. Common to these studies is the assumption that these biases are triggered by the formation of a decision. Our findings, however, extend this notion by suggesting that a similar micro-level evidence integration bias operates during decision formation, before committing to a choice (see also refs. [61,62]). In particular, we found that the best-fitting model was one in which the evidence is boosted for consistent evidence frames (this boost increases with the number of consecutive consistent frames) and is reset to baseline when the first inconsistent piece of evidence is encountered. Despite its evidence distortion, we have shown that this mechanism has an adaptive function in the presence of integration noise. Since evidence samples that are consistent with their predecessors are more likely to carry stronger evidence in favour of the correct alternative, inflating their weight provides extra protection from the corrupting effect of accumulation noise, resulting in increased decision accuracy (Fig. 6). This 'normativity hypothesis' predicts that, to the extent that consistency-based evidence integration is a controlled and adjustable strategy, consistency-sensitivity effects will increase as a function of integration noise, for example, when one is performing a dual task or when working memory is loaded. We leave this interesting question for future studies (see ref. [32] for a parallel investigation in relation to SI).

Our findings raise the intriguing hypothesis that confirmation biases are a form of consistency bias, whereby post-choice evidence

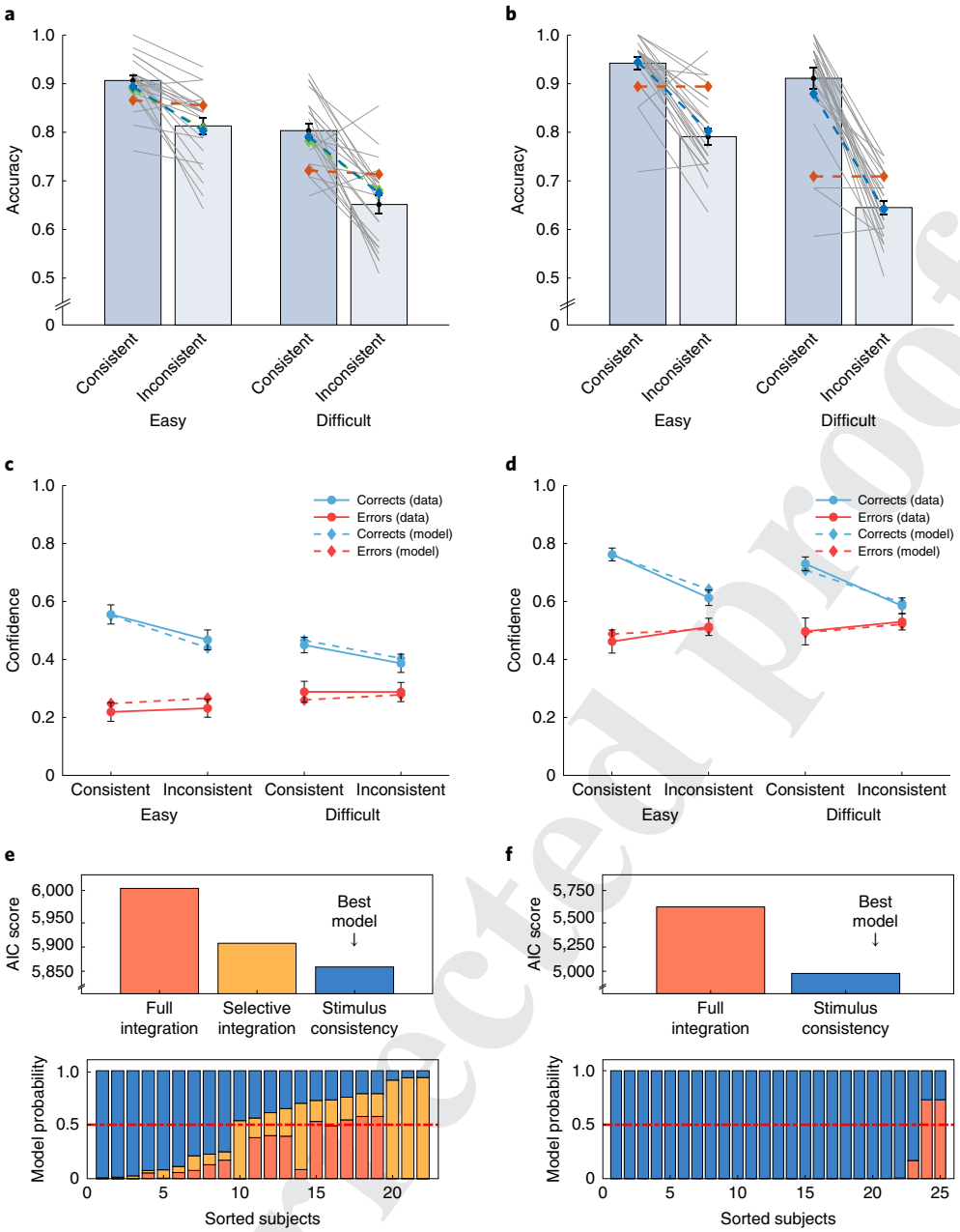


**Fig. 5 | Results of experiments 3 and 4. a**, Choice accuracy in experiment 3 as a function of difficulty (separation between the sampling distributions: easy versus difficult) and consistency (difference in the directions of the evidence: consistent versus inconsistent). The red, green and blue lines correspond to the predictions of the full/leaky-integration, SI and stimulus-consistency models, respectively. The thin grey lines correspond to individual participants ($n = 22$). **b**, Same as **a** for experiment 4. Note that, here, the predictions of the SI model were not included as only one stream of evidence was presented ($n = 25$ participants). **c**, Confidence as a function of difficulty and consistency for correct (blue lines) and incorrect (red lines) responses. Data are shown with solid lines and circle symbols. Model predictions are shown with dashed lines and diamond symbols ($n = 22$ participants). **d**, Same as **c** for experiment 4 ($n = 25$ participants). **e**, Model comparison for experiment 3. The stimulus-consistency model outperformed the leaky and SI models. **f**, Model comparison results for experiment 4. As in experiment 3, the stimulus-consistency model outperformed the integration model. Data are presented as mean ± s.e.m.

inconsistent with pre-choice evidence is integrated less effectively than post-choice consistent evidence. Future studies should investigate whether, to what extent and how consistency and confirmation biases are related, by measuring both biases within participants and using a unified paradigm. Another interesting possibility is that the consistency of evidence supporting a decision might affect the extent of a confirmation bias. For example, choices that are based on more consistent evidence may probably be more prone to confirmation bias, for example, due to the mediating effect of decision confidence[30]. Future studies could also beneficially examine whether and how consistency bias is related to a broad range of individual traits such as the need for cognitive closure[63], political radicalism[57] and dogmatism[64], or to psychiatric conditions such as obsessive compulsive disorder[65]. Consistency bias may be also related to higher-level judgements such as legal decisions, in which overweighting of consistent evidence may lead to erroneous decisions.

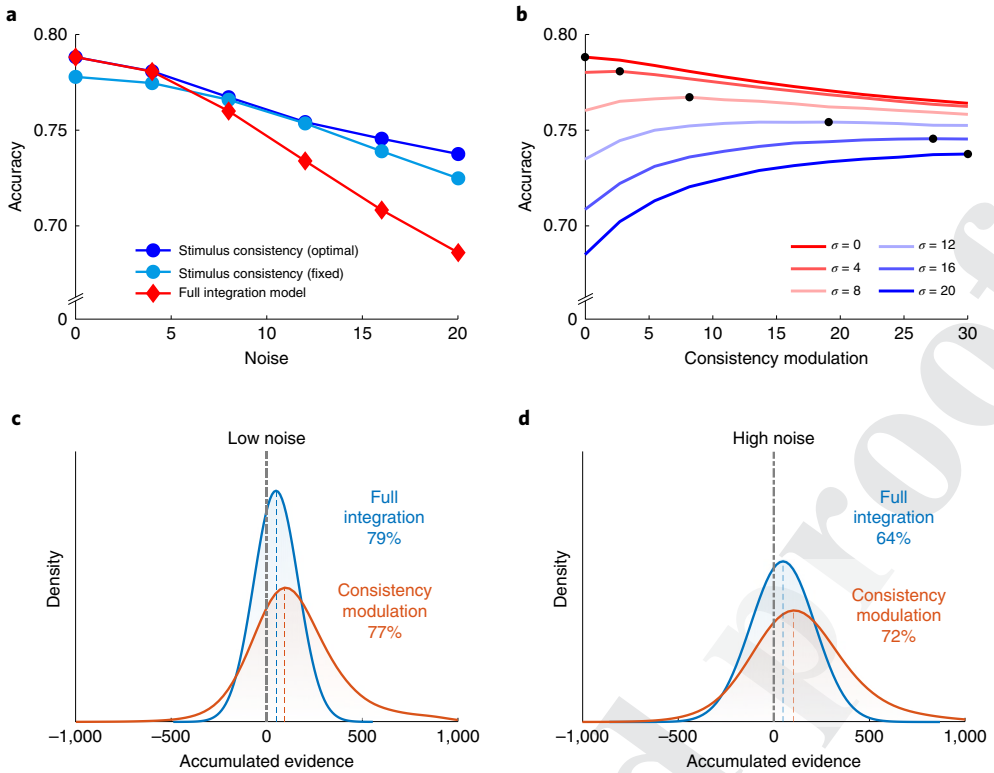


**Fig. 6 | Stimulus consistency and normativity. a**, Consistency-based modulation and normativity accuracy (that is, robustness to noise) as a function of noise, separately for the full-integration (red line) and stimulus-consistency models (blue lines). The accuracy of the stimulus-consistency model is presented for the model simulated using a fixed consistency parameter value of 10 (light blue) and for the model simulated using the optimal consistency parameter for each noise level (dark blue; see also **b**). **b**, Accuracy of the stimulus-consistency model as a function of the consistency-modulation strength, for different levels of noise ($\sigma$ curves). Black circles indicate consistency values that maximize the accuracy for a given level of accumulation noise. One can see that, as the level of the noise increases (red to blue lines), so does the level of consistency modulation needed to achieve the optimal performance (black circles). **c**,**d**, The distributions of the total accumulated evidence at the moment of response for the full-integration model (blue) and the stimulus-consistency model (red). The accuracy of the full integration model is higher than that of the stimulus-consistency model for low-noise simulations (**c**), but the stimulus-consistency model is more accurate for high-noise simulations (**d**).

We believe that our paradigm provides an important advantage over current confirmation bias paradigms by addressing these questions. In current confirmation bias paradigms, which probe one's ability to revise initially wrong decisions, validity might be jeopardized by demand characteristics (for example, presenting oneself in a self-consistent manner). In contrast, the current approach eschews these concerns, since participants are not required to contradict or confirm their previous decisions.

In conclusion, our methods allowed us to validate critical aspects of the evidence accumulation process and to unravel the biases that affect it. Our findings contribute to a growing literature speaking to the notion that self-inflicted distortions of evidence are ironically adaptive in that they act to increase choice veracity by making it robust to noise. A critical next step is to study how these strategies are acquired and how they relate to puzzling behaviours such as confirmation bias, and to better characterize the environmental and psychological variables that affect strategy selection.

## Methods

**Experimental methods.** *Participants.* The participants were undergraduates from Tel Aviv University: 27 (22 female, age 21–28 years) in experiment 1 (data taken from ref. [34]), 30 (22 female, age 18–35 years) in experiment 2, 23 (17 female, age 21–30 years) in experiment 3 and 25 (12 female, age 18–32 years) in experiment 4, all of whom reported having normal or corrected-to-normal vision. The participants in experiment 1, 2 and 3 received course credit in exchange for taking part in the experiments, as well as a bonus fee ranging from 15 to 25 ILS, which was determined by their task performance. The participants in experiment 4 were recruited via Prolific (https://prolific.ac/) and received £4 in exchange for participation. All experiments were approved by the ethics committee of Tel Aviv University.

*Stimuli.* The stimuli consisted of pairs of numerical values (experiments 1 and 3) or bars (experiment 2) which were presented simultaneously (Fig. 1a,b) at a rate of 2 Hz (500 ms per frame, experiments 1 and 3) or 5 Hz (200 ms per frame, experiment 2). In experiment 4, the stimuli consisted of a single stream of red and blue arrays of dots (Fig. 4b) presented at a rate of 12.5 Hz (80 ms per frame). Displays in experiments 1 and 3 were generated by an Intel I7 personal computer attached to an Asus 24" 248qe monitor with a refresh rate of 144 Hz using the 1,920 × 1,080 resolution graphics mode. Displays in experiment 2 were generated by an Intel I3 personal computer attached to a ViewSonic Graphics Series 19" G90fB CRT monitor with a refresh rate of 60 Hz using the 1,024 × 768 resolution graphics mode. Experiment 4 was designed in PsychoPy3[66] and hosted online using Pavlovia (http://www.pavlovia.org/). Responses were collected via the computer keyboard. The viewing distance was approximately 60 cm from the monitor.

*Task and design.* Each trial in the experiments began with a fixation display consisting of a black 0.2° × 0.2° fixation cross (+) that remained on the screen for 1 s. Then, pairs of numerical values (experiments 1 and 3), bars (experiment 2) or arrays of dots (experiment 4) were presented sequentially to the participants, who were asked to decide which sequence was drawn from a distribution with a higher mean value (experiment 1) or greater mean length (experiment 2), which of the sequences had a higher mean (experiment 3) or whether more blue or red dots were presented in total (experiment 4). The presentation in experiments 1 and 2 was terminated by the participants' response (free response protocol), whilst the presentation in experiments 3 and 4 was terminated after eight samples (interrogation protocol). In experiment 1, trials in which the response was faster than 250 ms or was performed after more than 11 samples were presented were excluded from further analysis (less than 2% of the data). In experiment 2, trials

in which the response was faster than 200 ms or performed after more than 20 samples were presented, or in which choice or decision confidence were not recorded were excluded from further analysis (less than 5% of the data). Responses were given by pressing the arrow keys (experiments 1 and 2; left/right arrow key for the left/right sequence, respectively) or by using the computer mouse (experiments 3 and 4). In experiments 2, 3 and 4, after indicating the sequence with the higher mean, participants were also asked to indicate their choice confidence. In experiment 2, we used a continuous scale with end points labelled '50%' and '100%'. In experiment 3, we used a six-button radio scale with end points (that is, 1 and 6) labelled 'Not confident at all' and 'Very confident'. In experiment 4, we used a continuous scale with end points labelled 'Not confident at all' and 'Very confident'. Confidence scores were normalized using min–max normalization:

$$\text{Normalized confidence} = \frac{\text{confidence} - \min(\text{confidence})}{\max(\text{confidence}) - \min(\text{confidence})}.$$

*Experimental conditions.* In all the experiments, the samples were drawn from Gaussians distributions. Experiment 1 included two difficulty levels, which were manipulated by varying the separation between the Gaussians: in the easy trials the means of the Gaussians were $\mu_1 = 52$ versus $\mu_2 = 44$, $\sigma = 10$, whilst in the difficult trials the means were $\mu_1 = 52$ versus $\mu_2 = 48$, $\sigma = 10$. Experiment 2 also consisted of two difficulty levels with $\mu_1 = 52.5$ versus $\mu_2 = 47.5$ and $\mu_1 = 51.5$ versus $\mu_2 = 48.5$, as well as an orthogonal manipulation of the sequences variance with $\sigma_1 = 0.1167$ versus $\sigma_2 = 0.07$. In experiment 3, we orthogonally manipulated the difficulty and the consistency of the evidence. Difficulty was manipulated by increasing the separation between the Gaussians from $\mu_1 = 52$ versus $\mu_2 = 48$, $\sigma = 10$ (difficult trials) to $\mu_1 = 52$ versus $\mu_2 = 44$, $\sigma = 10$ (easy trials). Consistency was manipulated by sampling eight values from the high- as well as from the low-mean distributions. Then, to generate consistent trials, we paired these values such that, in seven out of the eight pairs, the stronger evidence was in favour of the higher-mean distribution (Fig. 4c, lower panel). To generate inconsistent trials, we shuffled the temporal order of the same values and repaired them such that in only four out of the eight pairs was the stronger evidence in favour of the higher-mean distribution (Fig. 4c, upper panel). In experiment 4, difficulty and consistency were also orthogonally manipulated. Difficulty was manipulated by decreasing the mean of the Gaussian from $\mu = 5$ to $\mu = 2$ ($\sigma = 20$ in both conditions). Consistency was manipulated by generating two types of trials: consistent trials, in which seven out of the eight frames provided support for one of the alternatives (Fig. 4d, lower panel), and inconsistent trials, in which each alternative was supported by four of the frames (Fig. 4d, upper panel).

**Statistical analysis.** *Correlations and mean comparisons.* Correlations were examined using the Pearson correlation coefficient. Means were compared using permutation tests with $10^5$ random shuffles. All tests were two sided.

*Mixed effects models.* The effects of accumulated evidence and stimulus consistency on accuracy and RT confidence in experiments 1 and 2 (Table 1) were estimated on a trial-by-trial basis using mixed model regression analyses. The regressions were implemented using the MATLAB 'fitlme' and 'fitglme' functions with participants serving as random effects and with a free covariance matrix. The fixed effects variables were: (1) accumulated evidence, calculated as the sum of differences between the two streams of evidence at the moment of response, and (2) stimulus consistency, calculated as the absolute value of the difference between the number of frames with evidence favouring the two alternatives, normalized by the length of trial. Both variables were normalized using $z$ score transformations.

Choices in experiments 1 and 2 (coded as 1 for correct and 0 for error) were predicted using logistic regressions, which in Wilkinson notation was

$$\text{logit}\,(P_{\text{Choices}}) \sim (\text{accumulated evidence}) + (\text{stimulus consistency}) + (1|\text{subject})$$

RTs (experiments 1 and 2) and confidence (experiment 2) were predicted using linear regressions, which in Wilkinson notation were

$$\text{RT} \sim (\text{accumulated evidence}) + (\text{stimulus consistency}) + (1|\text{subject})$$

$$\text{Confidence} \sim (\text{accumulated evidence}) + (\text{stimulus consistency}) + (1|\text{subject})$$

The exact same pattern of results reported in Table 1 was obtained if the accumulated evidence and stimulus consistency were also included as random effects.

**Computational methods.** The validity of the model-free method was tested by simulating 10,000 synthetic decisions using known (fixed or collapsing) boundaries and examining the ability of the model-free method to accurately recover them. The values in all simulations (Fig. 2a–d) were sampled from $X \sim N(52, 15^2)$ and $Y \sim N(46, 15^2)$. The decision process in Fig. 2a,b was based on equation (1) with either a fixed (Fig. 2a) or collapsing boundary (Fig. 2b). The fixed boundary was characterized by a single boundary parameter ($c = 50$), and the collapsing boundary was characterized by four parameters describing the intercept, shape, scale and asymptote ($a = 100$, $k = 3$, $\lambda = 4$ and $a' = 10$; Computational methods and ref. [38]). The decision process in Fig. 2c,d was based on the value and difference cut-off heuristics with cut-offs of 70 and 20, respectively[34].

The decision boundaries in Fig. 2a–d were extracted by applying the LDA algorithm[39,40] to the integrated evidence excluding internal noise (that is, $Y(t)$, see equation (3)). For each frame ($t$), each trial that was not terminated before $t$ was classified as one of the following categories: choose alternative A, choose alternative B or continue sampling. Then, using the LDA, we extracted the planes that optimized the separation between different classes for each frame. We assumed that the upper and lower boundaries were symmetrical and therefore averaged both.

As mentioned in the main text, the internal noise causes an unavoidable overlap between the different classes. This overlap impairs the ability of the LDA to correctly extract the decision boundary and is particularly evident in slow trials due to the accumulation of internal noise across time[67]. Thus, to increase the robustness of the model-free method to internal noise, we constrained the boundary extraction of each frame by previous ones. To this end, we extracted the boundary based on two predictors: $t$ and $Y(t)$, as illustrated in the table below:

The LDA algorithm provides linear functions that separate the different classes from each other. To obtain the value of the boundary for the $n$th frame, we computed the value of the separating linear functions for this frame.

**Modelling details.** *Integration-to-boundary models.* We examined several integration-to-boundary models, all of them assuming integration of evidence based on the formula

$$X(t) = X(t-1) + \mu(t) + \varepsilon(t), \varepsilon \sim N\left(0, \sigma^2\right),$$

where $X(t)$ is the accumulated differences at time $t$ and $\varepsilon(t)$ is a random Gaussian noise, which is independent from the evidence-sampling noise. The term $\mu(t)$ varied between the different models as follows:

Full integration.

$$\mu(t) = V_{\text{L}}(t) - V_{\text{R}}(t), \tag{3}$$

where $V_{\text{L}}(t)$ and $V_{\text{R}}(t)$ are the samples drawn from the left and right distributions at time $t$, respectively (note that $V_{\text{L}}(t)$ and $V_{\text{R}}(t)$ include the sampling noise).

Stimulus consistency.

$$\mu(t) = V_{\text{L}}(t) - V_{\text{R}}(t) + \text{sign}\left(V_{\text{L}}(t) - V_{\text{R}}(t)\right) \times \theta \times i, \tag{4}$$

where $\theta$ is a free parameter representing the enhancement given to pieces of evidence that are consistent with previous ones and $i$ counts the run of consistent values (starting at 0). For example, if the differences between the values are 15, 20, 8, −15 and −25, then $i_{t=1} = 0$, $i_{t=2} = 1$, $i_{t=3} = 2$, $i_{t=4} = 0$ and $i_{t=5} = 1$.

Preference consistency.

$$\mu(t) = \begin{cases} \left(V_{\text{L}}(t) - V_{\text{R}}(t)\right) \cdot \theta, & \text{if} \frac{\text{sign}\left(V_{\text{L}}(t) - V_{\text{R}}(t)\right)}{\text{sign}\left(X(t-1)\right)} = 1 \\ V_{\text{L}}(t) - V_{\text{R}}(t), & \text{otherwise} \end{cases} \tag{5}$$

where $\theta$ is a free parameter representing the enhancement given to pieces of evidence consistent with the total accumulated evidence at time $t-1$.

Selective integration.

$$\mu(t) = V_{\text{L}}(t) \cdot \frac{1}{1 + e^{-\theta\left(V_{\text{L}}(t) - V_{\text{R}}(t)\right)}} - V_{\text{R}}(t) \cdot \frac{1}{1 + e^{-\theta\left(V_{\text{R}}(t) - V_{\text{L}}(t)\right)}}, \tag{6}$$

where $\theta$ is a free parameter affecting the magnitude of the selective gating[23].

All the integration models in experiments 1 and 2 assume integration to a collapsing boundary[34], modelled using a Weibull cumulative distribution function:[38]

$$u(t) = a - \left[1 - \exp\left(-\left(\frac{t}{\lambda}\right)^k\right)\right] \cdot \left(a - a'\right), \tag{7}$$

where $\pm u(t)$ are the upper/lower thresholds at time $t$, $a/a'$ are the initial (intercept) and asymptotic values of the boundary, respectively, and $\lambda$ and $k$ are the scale and shape parameters of the Weibull function, respectively.

In experiments 3 and 4, we used an interrogation paradigm, in which the probability of choosing each alternative was calculated using an exponential version of Luce's choice rule:[68]

$$\begin{aligned} P(\text{left}) &= \frac{1}{1 + e^{-\left(\beta_0 + \beta_1\left(\sum_{t=1}^{n} \mu(t)\right)\right)}} \\ P(\text{right}) &= 1 - P(\text{left}) \end{aligned}, \tag{8}$$

where $\beta_1$ indicates the sensitivity of the model to the accumulated evidence, with an intercept of $\beta_0$.

Q16 In addition, we examined whether the participants in experiments 3 and B showed a recency bias, as reported in several previous studies which used an interrogation paradigm[33,53]. To this end, for each participant, we performed a temporal logistic regression analysis, in which we predicted the response of each trial based on the differences between $V_L$ and $V_R$ at each frame, ranked by their temporal order. In experiment 3, the mean weight of samples 5–8 was significantly higher than that of samples 1–4 (permutation test, $P<0.001$, Cohen's $d=2.09$, 95% CI 0.30–0.45), indicating a recency bias. No such effect was found in experiment 4 ($P=0.09$, Cohen's $d=0.35$, 95% CI −0.01 to 0.10). This motivated us to include a leak term in experiment 3 (ref. [10]), which controls the extent to which earlier values are given less weight. Thus, equation (8) was extended to the following form in experiment 3:

$$P(\text{left}) = \frac{1}{1+e^{-\left(\beta_0+\beta_1\left((1-\lambda)^{n-t}\cdot\sum_{i=1}^{n}\mu(i)\right)\right)}}, \qquad P(\text{right}) = 1 - P(\text{left}) \tag{9}$$

where $\lambda$ is the leak term.

*Non-integration-to-boundary models.* We examine three models that did not assume integration of evidence-decision boundary (Figs. 1c,d and 2c,d). The first model is the value cut-off heuristic, which assumes that observers choose based on the detection of a single high-value sample. For example, if a participant uses a cut-off value of 70, then they will choose the sequences in which a value higher than 70 first appears. The second heuristic is the difference cut-off heuristic, which assumes that observers choose based on the first frame in which the difference between the numbers exceeds a predetermined threshold[34]. In addition to these two heuristics, we examined a third model which we labelled a random-timer model. This model assumes integration of evidence based on equation (1), but the RT is determined by an exogenous process. The value cut-off heuristic was simulated using a threshold of 70 (experiment 1, Fig. 1c), 80 (experiment 2, Fig. 1d) and 70 (model free, Fig. 2c). The difference cut-off heuristic was simulated using a threshold of 20 (experiment 1, Fig. 1c), 25 (experiment 2, Fig. 1d) and 20 (model free, Fig. 2d). The RTs of the random timer model were sampled from an ex-Gaussian distribution with $\mu=3$, $\sigma=0.5$ and $\lambda=2/3$ (experiment 1, Fig. 1c) and $\mu=6$, $\sigma=1$ and $\lambda=3$ (experiment 2, Fig. 2c). These values were chosen because they provided accuracy and RTs similar to the ones observed in the data of experiments 1 and 2.

*Optimization procedure.* The free parameters of the computational models were fitted to the data (choices and decision times) of each participant in experiments 1 and 2 separately, using maximum likelihood estimation. For each trial, we simulated the different models 1,000 times for a given set of proposal parameters and calculated the proportion of trials in which the model choice and decision time matched the empirical data. Denoting the proportion of match between the simulated and empirical data by $_{pi}$, we maximized the likelihood function $L(D|\theta)$ of the data ($D$) given a set of proposal parameters ($\theta$), by

$$L(D|\theta) = \prod_{i=1}^{N} p_i.$$

To find the best set of proposal parameters, we first used an adaptive grid search algorithm (see ref. [69] for details) and then used the three best sets of proposal parameters as starting points to a simplex minimization routine[70]. This data fitting procedure showed good to excellent ability[71] to recover the free parameters of the models (Supplementary Figs. 8 and 9).

**Reporting summary.** Further information on research design is available in the Nature Research Reporting Summary linked to this article.

## Data availability

The data that support the findings of this paper are available at https://osf.io/vywbx/.

## Code availability

The codes used for all studies are available at https://osf.io/vywbx/.

Received: 12 October 2020; Accepted: 11 February 2022;

## References

1. Bogacz, R., Brown, E., Moehlis, J., Holmes, P. & Cohen, J. D. The physics of optimal decision making: a formal analysis of models of performance in two-alternative forced-choice tasks. *Psychol. Rev.* **113**, 700–765 (2006).
2. Gold, J. I. & Shadlen, M. N. Banburismus and the brain: decoding the relationship between sensory stimuli, decisions, and reward. *Neuron* **36**, 299–308 (2002).
3. Moran, R. Optimal decision making in heterogeneous and biased environments. *Psychon. Bull. Rev.* **22**, 38–53 (2015).
4. Wald, A. Foundations of a general theory of sequential decision functions. *Econometrica* **15**, 279 (1947).
5. Forstmann, B. U., Ratcliff, R. & Wagenmakers, E. J. Sequential sampling models in cognitive neuroscience: advantages, applications, and extensions. *Annu. Rev. Psychol.* **67**, 641–666 (2016).
6. Brown, S. D. & Heathcote, A. The simplest complete model of choice response time: linear ballistic accumulation. *Cogn. Psychol.* **57**, 153–178 (2008).
7. Gold, J. I. & Shadlen, M. N. Neural computations that underlie decisions about sensory stimuli. *Trends Cogn. Sci.* **5**, 10–16 (2001).
8. Ratcliff, R. & McKoon, G. The diffusion decision model: theory and data for two-choice decision tasks. *Neural Comput.* **20**, 873–922 (2008).
9. Teodorescu, A. R. & Usher, M. Disentangling decision models: from independence to competition. *Psychol. Rev.* **120**, 1–38 (2013).
10. Usher, M. & McClelland, J. L. The time course of perceptual choice: the leaky, competing accumulator model. *Psychol. Rev.* **108**, 550–592 (2001).
11. Vickers, D. Evidence for an accumulator model of psychophysical discrimination. *Ergonomics* **13**, 37–58 (1970).
12. Wickelgren, W. A. Speed–accuracy tradeoff and information processing dynamics. *Acta Psychol. (Amst.).* **41**, 67–85 (1977).
13. Gold, J. I. & Shadlen, M. N. The neural basis of decision making. *Annu. Rev. Neurosci.* **30** (2007). Q17
14. Mulder, M. J., van Maanen, L. & Forstmann, B. U. Perceptual decision neurosciences – a model-based review. *Neuroscience* **277**, 872–884 (2014).
15. Latimer, K. W., Yates, J. L., Meister, M. L. R., Huk, A. C. & Pillow, J. W. Single-trial spike trains in parietal cortex reveal discrete steps during decision-making. *Sci. (80-.).* **349**, 184–187 (2015).
16. Watson, A. B. Probability summation over time. *Vis. Res.* **19**, 515–522 (1979).
17. Stine, G. M., Zylberberg, A., Ditterich, J. & Shadlen, M. N. Differentiating between integration and non-integration strategies in perceptual decision making. *eLife* **9** (2020).
18. Balci, F. et al. Acquisition of decision making criteria: reward rate ultimately beats accuracy. *Attention Percept. Psychophys.* **73**, 640–657 (2011).
19. Bogacz, R., Hu, P. T., Holmes, P. J. & Cohen, J. D. Do humans produce the speed-accuracy trade-off that maximizes reward rate? *Q. J. Exp. Psychol.* **63**, 863–891 (2010).
20. Palestro, J. J., Weichart, E., Sederberg, P. B. & Turner, B. M. Some task demands induce collapsing bounds: evidence from a behavioral analysis. *Psychon. Bull. Rev.* **25**, 1225–1248 (2018).
21. Ditterich, J. Evidence for time-variant decision making. *Eur. J. Neurosci.* **24**, 3628–3641 (2006).
22. Voskuilen, C., Ratcliff, R. & Smith, P. L. Comparing fixed and collapsing boundary versions of the diffusion model. *J. Math. Psychol.* **73**, 59–79 (2016).
23. Glickman, M., Tsetsos, K. & Usher, M. Attentional selection mediates framing and risk-bias effects. *Psychol. Sci.* **29**, 2010–2019 (2018).
24. Glickman, M. et al. The formation of preference in risky choice. *PLoS Comput. Biol.* **15**, e1007201 (2019).
25. Gluth, S., Kern, N., Kortmann, M. & Vitali, C. L. Value-based attention but not divisive normalization influences decisions with multiple alternatives. *Nat. Hum. Behav.* **4**, 634–645 (2020).
26. Krajbich, I., Armel, C. & Rangel, A. Visual fixations and the computation and comparison of value in simple choice. *Nat. Neurosci.* **13**, 1292–1298 (2010).
27. Brehm, J. W. Postdecision changes in the desirability of alternatives. *J. Abnorm. Soc. Psychol.* **52**, 384–389 (1956).
28. Bronfman, Z. Z. et al. Decisions reduce sensitivity to subsequent information. *Proc. R. Soc. B* **282**, 20150228 (2015).
29. Kappes, A., Harvey, A. H., Lohrenz, T., Montague, P. R. & Sharot, T. Confirmation bias in the utilization of others' opinion strength. *Nat. Neurosci.* **23**, 130–137 (2020).
30. Rollwage, M. et al. Confidence drives a neural confirmation bias. *Nat. Commun.* **11**, 1 (2020).
31. Talluri, B. C., Urai, A. E., Tsetsos, K., Usher, M. & Donner, T. H. Confirmation bias through selective overweighting of choice-consistent evidence. *Curr. Biol.* **28**, 3128–3135.e8 (2018).
32. Spitzer, B., Waschke, L. & Summerfield, C. Selective overweighting of larger magnitudes during noisy numerical comparison. *Nat. Hum. Behav.* **1**, 1 (2017).
33. Tsetsos, K. et al. Economic irrationality is optimal during noisy decision making. *Proc. Natl Acad. Sci. USA* **113** (2016).
34. Glickman, M. & Usher, M. Integration to boundary in decisions between numerical sequences. *Cognition* **193**, 104022 (2019).
35. Thura, D. & Cisek, P. Modulation of premotor and primary motor cortical activity during volitional adjustments of speed-accuracy trade-offs. *J. Neurosci.* **36** (2016).
36. Thura, D. & Cisek, P. The basal ganglia do not select reach targets but control the urgency of commitment. *Neuron* **95**, 1160–1170.e5 (2017).
37. van Maanen, L., Fontanesi, L., Hawkins, G. E. & Forstmann, B. U. Striatal activation reflects urgency in perceptual decision making. *NeuroImage* **139** (2016).

38. Hawkins, G. E., Forstmann, B. U., Wagenmakers, E. J., Ratcliff, R. & Brown, S. D. Revisiting the evidence for collapsing boundaries and urgency signals in perceptual decision-making. *J. Neurosci.* **35**, 2476–2484 (2015).
39. Fisher, R. A. The use of multiple measurements in taxonomic problems. *Ann. Eugen.* **7**, 179–188 (1936).
40. McLachlan, G. J. *Discriminant Analysis and Statistical Pattern Recognition* (Wiley, 2005).
41. Dotan, D., Meyniel, F. & Dehaene, S. On-line confidence monitoring during decision making. *Cognition* **171**, 112–121 (2018).
42. Usher, M., Tsetsos, K., Glickman, M. & Chater, N. Selective integration: an attentional theory of choice biases and adaptive choice. *Curr. Dir. Psychol. Sci.* **28**, 552–559 (2019).
43. Zeigenfuse, M. D., Pleskac, T. J. & Liu, T. Rapid decisions from experience. *Cognition* **131**, 181–194 (2014).
44. Ossmy, O. et al. The timescale of perceptual evidence integration can be adapted to the environment. *Curr. Biol.* **23**, 981–986 (2013).
45. Roe, R. M., Busemeyer, J. R. & Townsend, J. T. Multialternative decision field theory: a dynamic connectionist model of decision making. *Psychol. Rev.* **108**, 370–392 (2001).
46. Balsdon, T., Wyart, V. & Mamassian, P. Confidence controls perceptual evidence accumulation. *Nat. Commun.* **11**, 1 (2020).
47. Eisen-Enosh, A., Farah, N., Burgansky-Eliash, Z., Polat, U. & Mandel, Y. Evaluation of critical flicker-fusion frequency measurement methods for the investigation of visual temporal resolution. *Sci. Rep.* **7**, 1 (2017).
48. Ludwig, C. J. H., Gilchrist, I. D., McSorley, E. & Baddeley, R. J. The temporal impulse response underlying saccadic decisions. *J. Neurosci.* **25**, 9907–9912 (2005).
49. Britten, K. H., Shadlen, M. N., Newsome, W. T. & Movshon, J. A. The analysis of visual motion: a comparison of neuronal and psychophysical performance. *J. Neurosci.* **12**, 4745–4765 (1992).
50. Shadlen, M. N. & Newsome, W. T. Neural basis of a perceptual decision in the parietal cortex (area LIP) of the rhesus monkey. *J. Neurophysiol.* **86**, 1916–1936 (2001).
51. Yang, T. & Shadlen, M. N. Probabilistic reasoning by neurons. *Nature* **447**, 1075–1080 (2007).
52. Luyckx, F., Spitzer, B., Blangero, A., Tsetsos, K. & Summerfield, C. Selective integration during sequential sampling in posterior neural signals. *Cereb. Cortex* **30**, 4454–4464 (2020).
53. Tsetsos, K., Chater, N. & Usher, M. Salience driven value integration explains decision biases and preference reversal. *Proc. Natl Acad. Sci. USA* **109** (2012).
54. Abrahamyan, A., Silva, L. L., Dakin, S. C., Carandini, M. & Gardner, J. L. Adaptable history biases in human perceptual decisions. *Proc. Natl Acad. Sci. USA* **113**, E3548–E3557 (2016).
55. Braun, A., Urai, A. E. & Donner, T. H. Adaptive history biases result from confidence-weighted accumulation of past choices. *J. Neurosci.* **38**, 2418–2429 (2018).
56. Urai, A. E., De Gee, J. W., Tsetsos, K. & Donner, T. H. Choice history biases subsequent evidence accumulation. *eLife* **8** (2019).
57. Rollwage, M., Dolan, R. J. & Fleming, S. M. Metacognitive failure as a feature of those holding radical beliefs. *Curr. Biol.* **28**, 4014–4021.e8 (2018).
58. Jazayeri, M. & Movshon, J. A. A new perceptual illusion reveals mechanisms of sensory decoding. *Nature* **446**, 912–915 (2007).
59. Luu, L. & Stocker, A. A. Post-decision biases reveal a self-consistency principle in perceptual inference. *eLife* **7** (2018).
60. Stocker, A. A. & Simoncelli, E. P. A Bayesian model of conditioned perception. *Adv. Neural Inf. Process. Syst.* **20**, 1409–1416 (2007).
61. Cheadle, S. et al. Adaptive gain control during human perceptual choice. *Neuron* **81**, 1429–1441 (2014).
62. Patai, Z. E. et al. Conflict detection in a sequential decision task is associated with increased cortico-subthalamic coherence and prolonged subthalamic oscillatory response in the beta band. Preprint at *bioRxiv* https://doi.org/10.1101/2020.06.09.141713 (2020).
63. Kruglanski, A. W. & Webster, D. M. Motivated closing of the mind: 'seizing' and 'freezing'. *Psychol. Rev.* **103**, 263–283 (1996).
64. Schulz, L., Rollwage, M., Dolan, R. J. & Fleming, S. M. Dogmatism manifests in lowered information search under uncertainty. *Proc. Natl Acad. Sci. USA* **117**, 31527–31534 (2020).
65. Cavedini, P., Gorini, A. & Bellodi, L. Understanding obsessive-compulsive disorder: focus on decision making. *Neuropsychol. Rev.* **16**, 3–15 (2006).
66. Peirce, J. et al. PsychoPy2: experiments in behavior made easy. *Behav. Res. Methods* **51**, 195–203 (2019).
67. Teodorescu, A. R., Moran, R. & Usher, M. Absolutely relative or relatively absolute: violations of value invariance in human decision making. *Psychon. Bull. Rev.* **23**, 22–38 (2016).
68. Luce, R. D. *Individual Choice Behavior: a Theoretical Analysis* (Chapman & Hall, 1959).
69. Tavares, G., Perona, P. & Rangel, A. The attentional drift diffusion model of simple perceptual decision-making. *Front. Neurosci.* **11**, 468 (2017).
70. Nelder, J. A. & Mead, R. A simplex method for function minimization. *Comput. J.* **7**, 308–313 (1965).
71. White, C. N., Servant, M. & Logan, G. D. Testing the validity of conflict drift–diffusion models for use in estimating cognitive processes: a parameter-recovery study. *Psychon. Bull. Rev.* **25**, 286–301 (2018).

## Acknowledgements

This research was supported by a grant to Marius Usher from the Israel Science Foundation (grant no. 1413/17). R.M. is a member of the Max Planck Centre for Computational Psychiatry and Ageing research at UCL, which is funded by the Max Planck Society, Munich, Germany (https://www.mpg.de/en, grant no. 647070403019). The funders had no role in study design, data collection and analysis, decision to publish or preparation of the manuscript. We thank B. Blain, I. Cogliati Dezza, L. Globig, C. Kelly, D. Lee, N. Nachman, T. Sharot and S. Zheng for critical reading of the manuscript and helpful comments.

## Author contributions

M.G and M.U. developed the study concept. M.G., R.M. and M.U. designed the experiments. M.G. and R.M. performed the experiments. M.G. analysed the data and carried out the computational modelling. M.G., R.M. and M.U. wrote the paper and contributed to data discussion and interpretation at all stages.

## Competing interests

The authors declare no competing interests.

## Additional information

**Supplementary information** The online version contains supplementary material available at https://doi.org/10.1038/s41562-022-01318-6.

**Correspondence and requests for materials** should be addressed to Moshe Glickman or Marius Usher.

**Peer review information** *Nature Human Behaviour* thanks Birte Forstmann, Redmond O'Connell and the other, anonymous, reviewer(s) for their contribution to the peer review of this work.

# QUERY FORM

| Nature Human Behaviour | |
|---|---|
| **Manuscript ID** | **[Art. Id: 1318]** |
| **Author** | **Moshe Glickman** |

**AUTHOR:**

The following queries have arisen during the editing of your manuscript. Please answer by making the requisite corrections directly in the e.proofing tool rather than marking them up on the PDF. This will ensure that your corrections are incorporated accurately and that your paper is published as quickly as possible.

| *Query No.* | *Nature of Query* |
|---|---|
| Q1: | Please check your article carefully, coordinate with any co-authors and enter all final edits clearly in the eproof, remembering to save frequently. Once corrections are submitted, we cannot routinely make further changes to the article. |
| Q2: | Note that the eproof should be amended in only one browser window at any one time; otherwise changes will be overwritten. |
| Q3: | Author surnames have been highlighted. Please check these carefully and adjust if the first name or surname is marked up incorrectly. Note that changes here will affect indexing of your article in public repositories such as PubMed. Also, carefully check the spelling and numbering of all author names and affiliations, and the corresponding email address(es). |
| Q4: | You cannot alter accepted Supplementary Information files except for critical changes to scientific content. If you do resupply any files, please also provide a brief (but complete) list of changes. If these are not considered scientific changes, any altered Supplementary files will not be used, only the originally accepted version will be published. |
| Q5: | If applicable, please ensure that any accession codes and datasets whose DOIs or other identifiers are mentioned in the paper are scheduled for public release as soon as possible, we recommend within a few days of submitting your proof, and update the database record with publication details from this article once available. |
| Q6: | In the sentence starting " More broadly, however, DCBs provide...." confirm the edit to "Results section". |
| Q7: | Tables have been renumbered in order to keep sequential ordering of Table cross-references in text. Please confirm if this is ok. |
| Q8: | In the sentence starting "First, to specify the evidence-integration mechanism..." define the abbreviation AIC. |
| Q9: | In the sentence starting "In addition to consistency, the difficulty of the trials.." confirm the addition of "N" for the distributions of the variables *Y*. |
| Q10: | Confirm Fig. 5b caption |
| Q11: | In the sentence starting "Future studies could also beneficially..." confirm the expansion of OCD (only used here). |
| Q12: | Check the sentence starting "In experiments 2, 3 and 4, after indicating the **sequence with the higher mean**" (was the higher mean queried in all three of these experiments?) |

# QUERY FORM

| Nature Human Behaviour | |
|---|---|
| **Manuscript ID** | **[Art. Id: 1318]** |
| **Author** | **Moshe Glickman** |

AUTHOR:

The following queries have arisen during the editing of your manuscript. Please answer by making the requisite corrections directly in the e.proofing tool rather than marking them up on the PDF. This will ensure that your corrections are incorporated accurately and that your paper is published as quickly as possible.

| *Query No.* | *Nature of Query* |
|---|---|
| Q13: | In the sentence starting "The fixed boundary was characterized by a single boundary parameter..." correct the self-referential citation to "Computational methods" section. Also, confirm the edit from "Hawkins et al. (2015)" to "ref. [38]" |
| Q14: | In the sentence starting “To this end, we extracted the boundary based on two predictors...” change "the table below" to a numerical table citation. |
| Q15: | Equations have been renumbered in order to keep sequential ordering of equation cross-references in text. Please confirm if this is ok. |
| Q16: | In the sentence starting “In addition, we examined whether-..”, confirm or correct “experiments 3 and B” |
| Q17: | In refs. 13, 17, 33, 35, 37, 53, 56 and 59, add page/article numbers. |
| Q18: | If ref. 62 (preprint) has now been published in final peer-reviewed form, please update the reference details if appropriate. |
| | |

nature research

Corresponding author(s): Moshe Glickman & Marius Usher

Last updated by author(s): Feb 3, 2022

# Reporting Summary

Nature Research wishes to improve the reproducibility of the work that we publish. This form provides structure for consistency and transparency in reporting. For further information on Nature Research policies, see our Editorial Policies and the Editorial Policy Checklist.

## Statistics

For all statistical analyses, confirm that the following items are present in the figure legend, table legend, main text, or Methods section.

| n/a | Confirmed | |
|---|---|---|
| ☐ | ☒ | The exact sample size (*n*) for each experimental group/condition, given as a discrete number and unit of measurement |
| ☐ | ☒ | A statement on whether measurements were taken from distinct samples or whether the same sample was measured repeatedly |
| ☐ | ☒ | The statistical test(s) used AND whether they are one- or two-sided<br>*Only common tests should be described solely by name; describe more complex techniques in the Methods section.* |
| ☐ | ☒ | A description of all covariates tested |
| ☐ | ☒ | A description of any assumptions or corrections, such as tests of normality and adjustment for multiple comparisons |
| ☐ | ☒ | A full description of the statistical parameters including central tendency (e.g. means) or other basic estimates (e.g. regression coefficient) AND variation (e.g. standard deviation) or associated estimates of uncertainty (e.g. confidence intervals) |
| ☐ | ☒ | For null hypothesis testing, the test statistic (e.g. *F*, *t*, *r*) with confidence intervals, effect sizes, degrees of freedom and *P* value noted<br>*Give P values as exact values whenever suitable.* |
| ☒ | ☐ | For Bayesian analysis, information on the choice of priors and Markov chain Monte Carlo settings |
| ☐ | ☒ | For hierarchical and complex designs, identification of the appropriate level for tests and full reporting of outcomes |
| ☐ | ☒ | Estimates of effect sizes (e.g. Cohen's *d*, Pearson's *r*), indicating how they were calculated |

*Our web collection on statistics for biologists contains articles on many of the points above.*

## Software and code

Policy information about availability of computer code

| | |
|---|---|
| Data collection | Experiments 1, 2 & 3 (in-lab experiments): Matlab R2017b (Mathworks, Inc.) and its Psychtoolbox extension (PTB-3). Experiment 4 (online experiment): designed in PsychoPy3 and hosted using Pavlovia. |
| Data analysis | Matlab R2017b (Mathworks, Inc.). |

For manuscripts utilizing custom algorithms or software that are central to the research but not yet described in published literature, software must be made available to editors and reviewers. We strongly encourage code deposition in a community repository (e.g. GitHub). See the Nature Research guidelines for submitting code & software for further information.

## Data

Policy information about availability of data

All manuscripts must include a data availability statement. This statement should provide the following information, where applicable:

- Accession codes, unique identifiers, or web links for publicly available datasets
- A list of figures that have associated raw data
- A description of any restrictions on data availability

The data that support the findings of this study are available at https://osf.io/vywbx/

# Field-specific reporting

Please select the one below that is the best fit for your research. If you are not sure, read the appropriate sections before making your selection.

☐ Life sciences ☒ Behavioural & social sciences ☐ Ecological, evolutionary & environmental sciences

For a reference copy of the document with all sections, see nature.com/documents/nr-reporting-summary-flat.pdf

# Behavioural & social sciences study design

All studies must disclose on these points even when the disclosure is negative.

| | |
|---|---|
| Study description | Quantitative experimental study. |
| Research sample | Research sample of experiments 1, 2 & 3 was consisted of Tel Aviv university undergraduate students: N=27 (Exp. 1; age range: 21-28, 22 females - the data in this study were taken from Glickman & Usher, 2019), N=30 (Exp. 2; age range: 18-35, 22 females) & N=22 (Exp. 3; age range: 21-30, 17 females). Research sample of experiments 1, 2 & 3 was consisted of Participants received course credit in exchange for taking part in the experiments, as well as a bonus fee ranging from 15 – 25 ILS (approximately $5-8), which was determined by their task performance. Research sa,mple of experiment 4 was consisted of participants recruited via Prolific (N = 25, age range: 18-32, 12 females) and received £4 in exchange for participation. We used non-probability sampling, as we studied basic decision mechanisms that should not vary with demographic factors. We used sample sizes of 20-30 participants for each experiment based on the effect sizes obtained in pilot experiments, and based on comparable published studies using similar paradigms, as for instance in:<br>1. Spitzer, B., Waschke, L., & Summerfield, C. (2017). Selective overweighting of larger magnitudes during noisy numerical comparison. Nature Human Behaviour, 1(8), 1-8.<br>2. Tsetsos, K., Moran, R., Moreland, J., Chater, N., Usher, M., & Summerfield, C. (2016). Economic irrationality is optimal during noisy decision making. Proceedings of the National Academy of Sciences, 113(11), 3102-3107. |
| Sampling strategy | See above. |
| Data collection | Data was collected using computerized behavioral tasks. In experiments 1, 2 & 3, participants were alone in the testing room and the researcher assistant remained in an adjacent room. Experiment 4 was conducted online. Participants and research assistants were blind to the hypotheses of the study. |
| Timing | 2013-2021 |
| Data exclusions | Data exclusions are described in the main text. |
| Non-participation | No participants dropped out or declined participation. |
| Randomization | All studies were conducted within-subject. Experimental conditions were inter-mixed. |

# Reporting for specific materials, systems and methods

We require information from authors about some types of materials, experimental systems and methods used in many studies. Here, indicate whether each material, system or method listed is relevant to your study. If you are not sure if a list item applies to your research, read the appropriate section before selecting a response.

## Materials & experimental systems

| n/a | Involved in the study |
|---|---|
| ☒ | ☐ Antibodies |
| ☒ | ☐ Eukaryotic cell lines |
| ☒ | ☐ Palaeontology and archaeology |
| ☒ | ☐ Animals and other organisms |
| ☐ | ☒ Human research participants |
| ☒ | ☐ Clinical data |
| ☒ | ☐ Dual use research of concern |

## Methods

| n/a | Involved in the study |
|---|---|
| ☒ | ☐ ChIP-seq |
| ☒ | ☐ Flow cytometry |
| ☒ | ☐ MRI-based neuroimaging |

## Human research participants

Policy information about studies involving human research participants

| | |
|---|---|
| Population characteristics | Young healthy adults, all had normal or corrected-to-normal vision. |

| | |
|---|---|
| Recruitment | Participants in experiments 1, 2 & 2 were recruited through the subject pool of Tel Aviv University. Participants in experiment 4 were recruited via Prolific. |
| Ethics oversight | The experiment was approved by the ethics committee at Tel-Aviv University, consent was given by a written form. |

Note that full information on the approval of the study protocol must also be provided in the manuscript.